Acoustical Physics, Vol. 49, No. 1, 2003, pp. 81–87. Translated from Akusticheskiĭ Zhurnal, Vol. 49, No. 1, 2003, pp. 92–99.
Original Russian Text Copyright © 2003 by Lebedev, Ostrovskiĭ, Sutin, Soustova, Johnson.

Resonant Acoustic Spectroscopy at Low *Q* Factors

A. V. Lebedev[1], L. A. Ostrovskiĭ[1, 2], A. M. Sutin[1, 3], I. A. Soustova[1], and P. A. Johnson[4]

[1] *Institute of Applied Physics, Russian Academy of Sciences, ul. Ul'yanova 46, Nizhni Novgorod, 603950 Russia*
e-mail: soustova@hydro.appl.sci-nnov.ru

[2] *Zel Technologies/NOAA Environmental Technology Laboratory, 325 Broadway, Boulder, Colorado 80305, USA*

[3] *Davidson Laboratory, Stevens Institute of Technology, 711 Hudson Street, Hoboken, NJ 07030, USA*

[4] *Los Alamos National Laboratory, Los Alamos, New Mexico 87501, USA*

Received August 26, 2002

Abstract—The application of resonant acoustic spectroscopy to rock, building materials, and materials with cracks is hindered by the substantial mechanical losses in these materials and by the overlapping of the individual resonance responses. The paper describes a method for the determination of the resonance frequencies in low-*Q* materials in the presence of a strong overlapping of resonances. The effect of cracks on the values of the resonance frequencies and *Q* factors is studied experimentally. *© 2003 MAIK "Nauka/Interperiodica".*

Resonant acoustic spectroscopy (RAS) has received wide acceptance as a method for measuring the elasticity tensors of various samples [1]. A detailed description of RAS methods along with examples of their application can be found in [1–3]. The high accuracy of this technique has made it a popular instrument for solving a wide variety of problems. For example, RAS is used for analyzing such effects and parameters as dissipation mechanisms in solids [4], phase transitions in superconducting materials [5], the mobility of dislocations in a crystal lattice [6], the structures of polycrystalline bodies [7] and composites [8], the effect of the treatment of a material on its microstructure [9], and the elastic moduli of the third order [10]; RAS is also used for estimating the grain size in a structurally inhomogeneous medium [11]. One of the most important areas of application of RAS is the nondestructive testing of materials [12–14].

Initially, RAS methods were developed for measuring the properties of crystals, e.g., for the determination of the specific heat of crystals or the detection of phase transitions in them. Such samples are almost free of internal defects, and, hence, the mechanical losses in them are small. Each resonance observed on these samples manifests itself as a sharp peak. The position of each peak in the frequency spectrum of the response determines a resonance frequency, and the width of the peak indicates the *Q* factor. This method of measuring the resonance frequencies and the *Q* factors enjoys wide application [1].

As for the resonant acoustic spectroscopy of composite and structurally inhomogeneous materials, the main obstacle here is the overlapping of individual resonance responses, which hinders the resolution of resonances and makes it impossible to obtain the required accuracy when using this method for nondestructive testing [15]. Unlike crystals, the composites and structurally inhomogeneous media (such as rock or building materials) are characterized by great numbers of internal defects and, hence, by high mechanical losses. As a result, the resonances do not manifest themselves as separate peaks, and the measurement of the resonance frequencies and *Q* factors by the conventional RAS technique is rather difficult. In the recent publication [16] (by one of the authors of this paper), the matched-filter processing of the experimental data was proposed as a method to determine the resonance frequencies and the *Q* factors in acoustic spectroscopy. In another publication [17], this method was shown to provide a high accuracy in measuring the elastic constants, including the cases when the conventional technique (the identification of the peaks) fails.

In the present paper, matched-filter processing is used to determine the resonance frequencies and the *Q* factors for materials with high concentrations of internal defects and to estimate the effect of cracks on the values of the resonance frequencies and *Q* factors at fracture. The first section briefly describes (on the basis of [16]) the method of the determination of the resonance frequencies and the *Q* factors of the samples; the second section describes the experimental setup and the scheme of measurements; and the third section discusses the results.

RESOLUTION OF OVERLAPPING RESONANCES

For the methods under consideration, the usual approach is the minimization of the mean square deviation of the measurement data from some selected physical model whose parameters are to be determined. In analyzing the linear response of a mechanical vibratory system with many degrees of freedom (modes), it is natural to choose a model in the form of the superposition of individual resonances. Then, the complex

1063-7710/03/4901-0081$24.00 © 2003 MAIK "Nauka/Interperiodica"

transfer function (TF) being defined as $\mathrm{TF}(\omega) = A_{\mathrm{out}}(\omega)/A_{\mathrm{inp}}(\omega)$, where $A_{\mathrm{inp}}(\omega)$ and $A_{\mathrm{out}}(\omega)$ are the complex amplitudes of the input and output signals proportional to the force and the displacement, respectively, should be represented in the form

$$\mathrm{TF}(p) = \sum_{l=1}^{M} A_l G(p, \delta_l, \omega_l). \quad (1)$$

Here, M is the number of resonances in the frequency range under consideration ($\omega_{\min} < \omega < \omega_{\max}$), $p = i\omega$, $G(p, \delta_l, \omega_l) = \dfrac{1}{p^2 + 2\delta_l p + \omega_l^2}$ is the response for the lth resonance, δ_l is the corresponding loss factor, and ω_l is the corresponding frequency. Function (1) describes the response of an arbitrary linear vibratory system in the frequency domain [18]. Let us assume that we know N values of the transfer function at the frequencies $p_n = i(\omega_{\min} + 2\pi\Delta f n/N)$, where $0 \le n \le N$, $\Delta f = (\omega_{\max} - \omega_{\min})/2\pi$ is the frequency range in which the experimental data are given, and $\Delta f/N$ is the frequency resolution of the transfer function. Then, the finite parameters of model (1), i.e., the number of resonances, their frequencies and amplitudes, and the loss factor, should provide the minimal mean square deviation of the measured (or given) values of $\mathrm{TF}_{\mathrm{exp}}(p_n)$ from the results of calculation by Eq. (1). We set the variations of the square magnitude of the corresponding difference with respect to A_l equal to zero to obtain a system of linear equations for the amplitudes of the responses:

$$C_{kl} A_l = D_k, \quad (2)$$

where $C_{kl} = \sum_{j=1}^{N} G^*(p_j, \delta_k, \omega_k) G(p_j, \delta_l, \omega_l)$ and $D_k = \sum_{j=1}^{N} G^*(p_j, \delta_k, \omega_k)\mathrm{TF}(p_j)$.

To determine the resonance frequencies ω_l and the loss factors δ_l in model (1), we use the modified methods of linear prediction in the time domain (see, e.g., [19]). To change from the frequency domain of definition of the transfer function to the time domain (the pulse response), we use a discrete Fourier transform, so that the array of equidistant readings in the frequency domain $\mathrm{TF}(p_n)$ is put in correspondence with an array of the readings ζ_n equidistant in time. The deviation of the predicted value of ζ_n from the measured one ζ_n^{exp} is minimized as follows [19]. We determine a characteristic polynomial $H(z) = 1 + \sum_{k=1}^{L} h_k z^{-k}$ with $z = \exp((-\delta + i\omega)/\Delta f)$. The polynomial coefficients represent the solution to the system of equations

$$a_{jk} h_k + b_j = 0, \quad (3)$$

where $a_{jk} = \zeta_{L-k+j}$, $b_j = \zeta_{L+j}$, $j = 1, 2, \ldots, N-L$, $k = 1, 2, \ldots, L$, and $L \ge M$. The zeros of the polynomial H [$H(z_l) = 0$, $z_l = \exp((-\delta_l + i\omega_l)/\Delta f)$] coincide with the poles of expression (1) (see [16, 19]). As a result, the mean square deviation of the measured data from the data obtained using model (1) with the corresponding set of parameters (ω_l, δ_l) and with the amplitudes A_l satisfying Eq. (2) proves to be minimal.

In the absence of losses ($\delta_l = 0$), the autocorrelation matrix $A = \hat{a}^+ \hat{a}$ [where $\hat{a} = a_{jk}$ is determined from Eqs. (3) and the sign $(\cdot)^+$ denotes Hermitian conjugation] has the dimension $L \times L$ and the rank M. The first M eigenvalues Λ of this matrix are positive ($\Lambda_k > 0$, $k = 1, 2, \ldots, M$), and the remaining $L - M$ eigenvalues are equal to zero: $\Lambda_k = 0$, $k = M+1, M+2, \ldots, L$ [19]. The presence of noise in the experimental data results in that the matrix A has a full rank. According to [19], the experimental data can be separated into the desired signal and the noise component by using the difference in the eigenvalues Λ_k: the small values of Λ_k should be identified with noise.

The presence of loss ($\delta_l \ne 0$) smoothes out the spectrum of the eigenvalues of the matrix A. In this case, the boundary between the desired signal (the contribution of resonances) and noise is assumed to be the break of the spectrum of Λ_k [16]. This allows one to determine the number M of the "true" resonances in model (1). If the signal-to-noise ratio (snr) is known or can be determined independently, the number of resonances can also be determined from the energy considerations (each Λ_k is equal to the power of the corresponding degree of freedom). Namely, for every (mth) physical resonance, the following condition should be met:

$$\mathrm{snr} \times \Lambda_m \ge \sum_{k=1}^{L} \Lambda_k. \quad (4)$$

The number of resonances M is determined as the maximal value of m satisfying inequality (4).

In this study, the number of resonances in the frequency band Δf is performed through the search for singularities in the spectrum of the eigenvalues Λ_k and the search for the maximal value of m in inequality (4). Then, after the value of M is determined, equations (3) and (2) are solved sequentially, and the parameters involved in model (1) are determined. The result of calculating the transfer function by Eq. (1) is compared with the experimental data. If discrepancies are obtained, the whole procedure is repeated with another value of L, which serves as the initial approximation for the number of resonances.

The measurement error for the parameters of model (1) is estimated in the conventional way. The goal function, which represents the sum of the squared magnitudes of the difference between the measured values of the transfer function and the parametric model (1), is represented as a Taylor series up to the

second-order terms for the values of A_l, ω_l, δ_l corresponding to the minimum of the goal function. In this case, the variance of each parameter of model (1) is determined by the ratio of the goal function to the second derivative of the goal function with respect to the corresponding parameter.

The proposed method was used to analyze the results of two series of measurements performed for materials with cracks. One series was performed for polycarbonate samples with the use of a swept signal, as in the case of the standard methods of resonant acoustic spectroscopy. The other series was performed for concrete samples with the use of impulse excitation of natural vibrations in the samples (impulse resonant spectroscopy). Note that no nonlinear effects were observed in the experiments described below.

RESONANT SPECTROSCOPY OF POLYCARBONATES

The polycarbonate samples had the form of rectangular bricks with the dimensions $13 \times 38 \times 132$ mm^3. Each sample had a 12-mm-deep groove. Under a cyclic loading, a visible crack was formed at the groove bottom. Sample no. 1 served as reference and was not subjected to loading, while sample no. 2 under the cyclic loading developed a 6-mm-long crack.

The measuring setup is schematically represented in Fig. 1. Piezoceramic transducers in the form of 2-mm-thick disks, 10 mm in diameter, were glued to the end surfaces of the sample. One of the transducers was used for the excitation of vibrations in the sample and the other served as a receiver. The response was measured by a resonant ultrasound spectroscope (produced by Dynamic Resonance Systems, see http://www.ndtest.com/). The setup made it possible to vary the excitation frequency and to save the data on the hard disk of a computer. The frequency resolution (the step in frequency) was 1 Hz in the frequency band 8–30 kHz and provided the possibility of recording the resonances with a Q factor up to 1000, which far exceeded the measured values of the Q factor.

Figure 2 presents the measured transfer function for a defect-free polycarbonate sample and the corresponding transfer function reconstructed by Eq. (1). One can see that, even for such a sample, the conventional analysis of the power spectral density (the search for peaks) does not allow one to determine all resonance frequencies and Q factors. Specifically, resonances marked in Fig. 2 by the numbers *3*, *7*, *9*, *12–15*, *17*, *18*, *20*, *22*, and *24* do not manifest themselves as peaks. Moreover, neither the amplitude nor the phase dependence of the transfer function on frequency provides the determination of the resonance positions with the use of only the local properties of TF(ω).

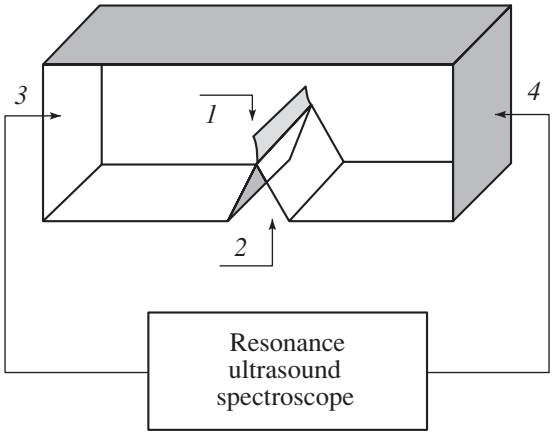

Fig. 1. Measuring setup: (*1*) crack, (*2*) groove, (*3*) position of the driving transducer, and (*4*) position of the receiver.

At the same time, the method discussed above provides the resolution of even noticeably overlapping resonance responses. To determine the number of resonances in the measuring frequency band, we performed the search for singularities (breaks) in the dependence $\Lambda(m)$ by using inequality (4). The value of the snr involved in inequality (4) was estimated as the ratio of the total spectral density (the sum of squared amplitudes) to the noise power in Fig. 2. The noise amplitude at every frequency was estimated as the difference between the measured value and the mean value obtained from the piecewise-linear smoothing approximation of the TF. The horizontal dashed line in Fig. 3 shows the noise power normalized to the total power of the signal. The intersection of this line with the curve corresponding to the eigenvalue spectrum normalized to the total power corresponds to the number of resonances in the measuring frequency band. The number of the resonances was found to be 29 within the frequency band 8–30 kHz. The Q factor of four resonances out of these 29 proved to be less than seven, which was much smaller than the mean value of the Q factor being approximately equal to 50. The appearance of these resonances was caused by the finite width of the measuring frequency band Δf and by the smooth trends arising in the frequency dependence of the TF. One resonance was found to have an amplitude comparable with the noise level and large errors in the measurements of its frequency and Q factor. Thus, the five resonances specified above were excluded from the analysis. The remaining $M = 24$ resonances are shown in Fig. 2. Their parameters were used for calculating the TF by Eq. (1).

It is well known that the presence of cracks mainly leads to a decrease in the Q factor while the propagation velocities of elastic waves vary within fractions of percent [20]. Since, initially, the Q factor values are small even for the defect-free sample, the measurement of the

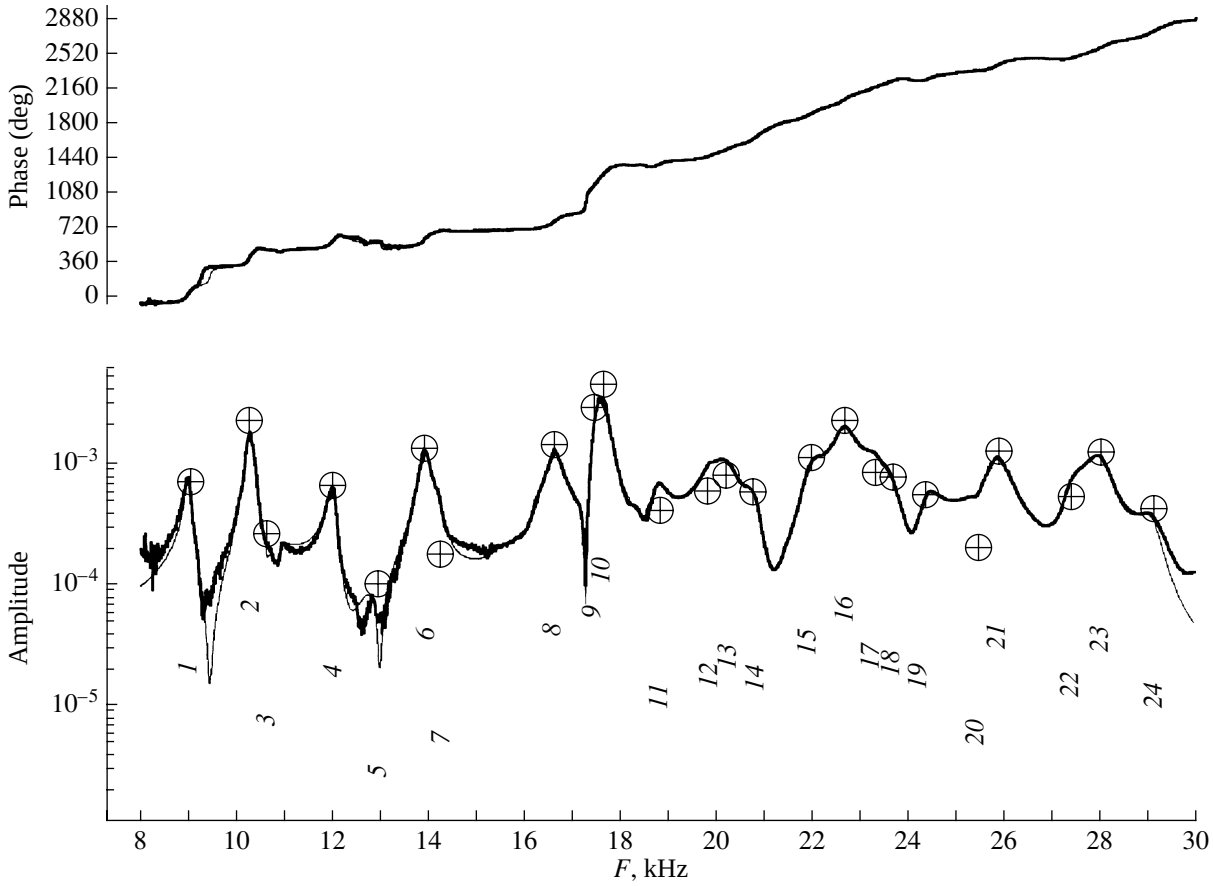

Fig. 2. Result of the reconstruction of the transfer function for sample 1 of polycarbonate (thin lines) and the experimental values of the TF (thick lines). The upper plot shows the phase and the lower plot, the amplitude of the TF.

Q factor variation due to the presence of cracks presents a difficult problem.

Figure 4 shows the resonance frequencies and the Q factors of the first ten resonances for polycarbonate samples 1 and 2. The frequencies were measured to within 1%, and the accuracy of the Q factor measurement was much lower. The maximal measurement errors were observed for the resonances whose amplitudes were comparable with the noise level (*1–3* in Fig. 2) and in the case of a considerable overlapping of the responses (*9* and *10* in Fig. 2). Of all resonances presented in Fig. 4, we can separate three, namely, the resonances marked by arrows (*6–8*) in Fig. 2, for which the measured values of the Q factor are statistically distinguishable (the confidence intervals of the data obtained for samples 1 and 2 do not overlap). The maximal variations in the resonance frequencies occur for the same three resonances *6–8* (Fig. 4). For these resonances, the appearance of the crack is accompanied by a loss increase. The Q factor decreases in the presence of the crack by approximately a factor of 2 with respect to the initial value ($Q_0 \approx 100$). The maximal changes in the Q factor are observed for the mode with the maximal initial Q factor value (mode *6* in Fig. 4).

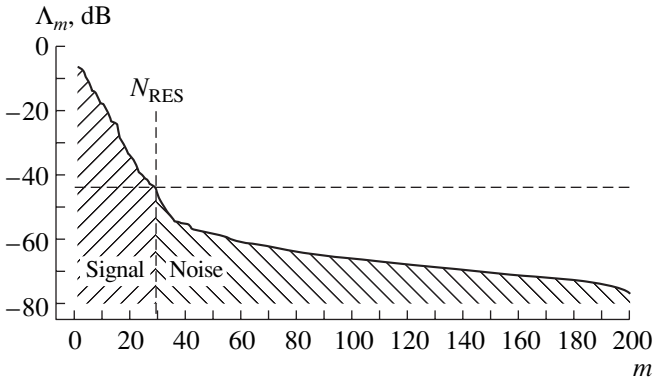

Fig. 3. Spectrum of the eigenvalues of the autocorrelation matrix for sample 1 of polycarbonate; the spectrum is normalized to the total power.

IMPULSE RESONANT SPECTROSCOPY OF CONCRETE SAMPLES

The second series of measurements was performed on two concrete samples. The samples had the form of rectangular bricks with the dimensions $152.4 \times 152.4 \times$

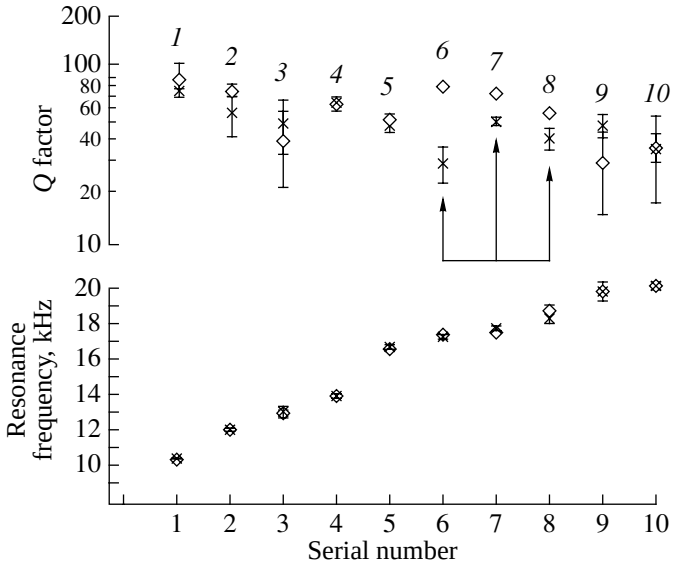

Fig. 4. Variations in the resonance frequencies and *Q* factors for the defect-free polycarbonate sample 1 and for sample 2 with a crack. The serial numbers of resonances correspond to the numbers given in Fig. 2. The measurement errors are shown by vertical segments, which correspond to the 60% confidence intervals under the assumption that the random noise is Gaussian. The diamonds (◇) refer to sample 1, and the crosses (×), to sample 2.

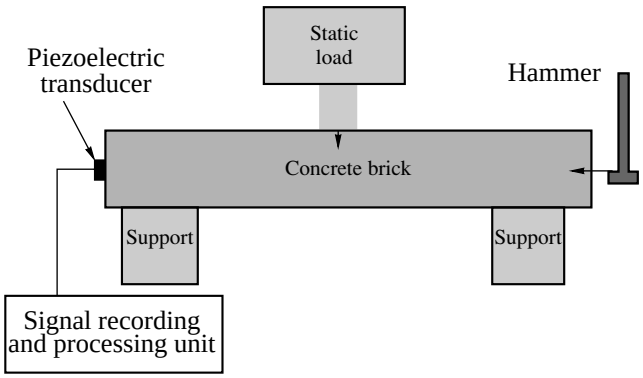

Fig. 5. Experimental setup.

533.4 mm^3 and had no grooves. Both samples initially had no defects and were gradually destroyed by a linearly increasing load until their fracture. The experimental setup is illustrated in Fig. 5.

The natural vibrations of the sample were excited by a small hammer. The latter performed a single stroke, which was controlled by a piezoceramic transducer mounted on the hammer.

Figure 6 presents examples of signal records after the stroke for a defect-free concrete brick and for a brick under the effect of a load causing the formation of microcracks. One can see that, in the brick with cracks, the increased losses lead to a faster damping of the excited vibrations.

The vibration excitation by a hammer stroke along the sample axis mainly resulted in the excitation of longitudinal vibrations. In the reconstruction of the TF for a concrete sample containing no defects, we obtained the peak corresponding to the lowest mode of longitudinal vibrations of the concrete brick (this mode is observed against the minimal noise level). As the sample was gradually destroyed, the peak was split, and the splitting increased with increasing load (Fig. 7).

Figure 8 shows this splitting as a function of the load applied to the sample. The breaking force in Fig. 7 is normalized in such a way that zero corresponds to the absence of load while unity, to the maximal value of the force beyond which the sample fracture takes place. The splitting of the peak is presumably related to the formation of cracks. The cracks were formed in the region of the maximal axial tension under the load (when the force was close to maximal, the cracking could be detected visually). Without discussing the mechanism of the splitting (it will be the subject of our subsequent studies), we note that the appearance of inhomogeneities inside the sample evidently leads to an increase in the number of eigenmodes (longitudinal or flexural), and one of the factors responsible for this effect is the elimination of the degeneracy related to the square cross section of the brick. Figure 9 shows the dependence of the *Q* factor of longitudinal vibrations

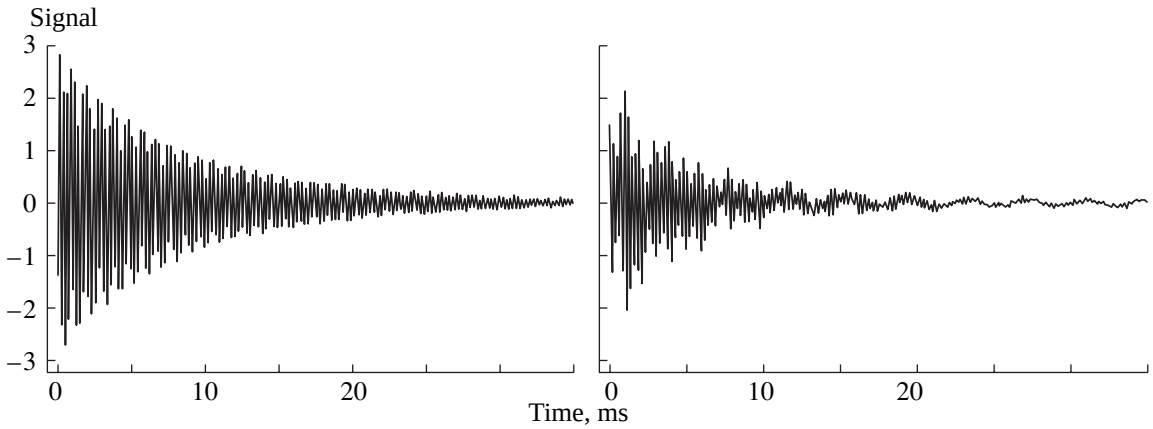

Fig. 6. Responses of concrete samples to a hammer stroke: the left plot refers to the defect-free sample and the right plot, to the sample immediately before fracture.

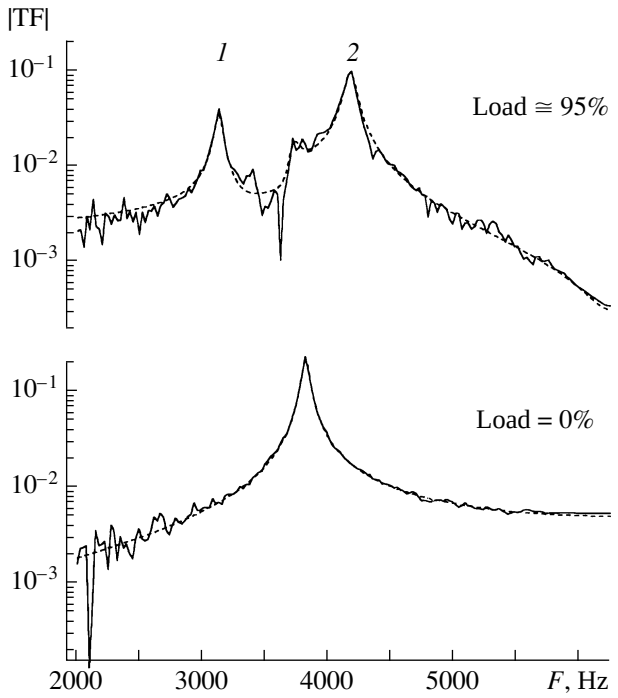

Fig. 7. Splitting of the peak under an increasing load; the peak corresponds to the longitudinal mode. The dashed lines show the result of the reconstruction of the frequency response by Eq. (1). (The peak numbers correspond to those in Fig. 8.)

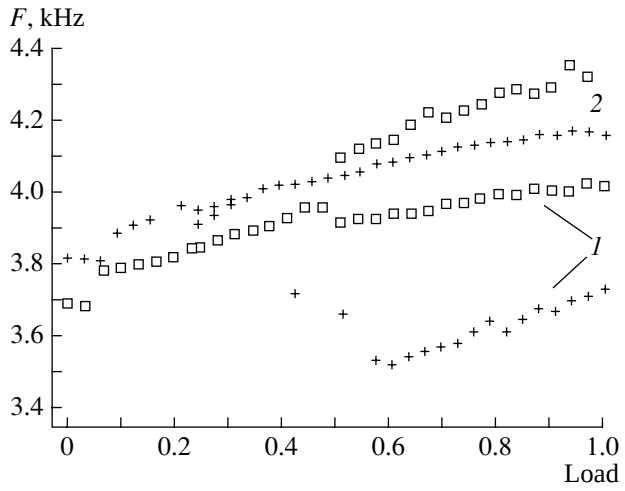

Fig. 8. Dependence of the resonance frequencies on the relative value of the breaking load for two peaks (*1* and *2*). The difference between samples 1 and 2 is determined by the difference in the material parameters of concrete of which they are made. The crosses (+) refer to sample 1 and the squares (□), to sample 2.

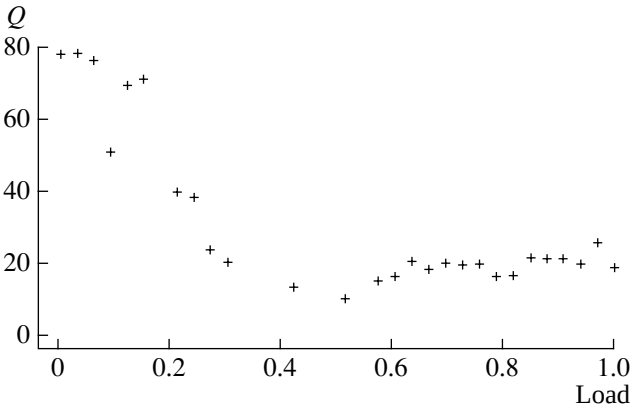

Fig. 9. Dependence of the *Q* factor of longitudinal vibrations on the relative value of the breaking load. The measurement error for the *Q* factor does not exceed 10.

(crosses in Fig. 8 and peak *1* in Fig. 7) on the breaking load. The data presented in Fig. 9 are obtained from the measurements on sample 1, which were performed with the highest accuracy. The data shown in Fig. 9 testify to the rapid decrease in the *Q* factor, starting from loads of about 10–20% of the ultimate load.

In the experiment, we observed a brittle fracture of concrete. It is expedient to compare our results with other data on the brittle fracture of solids. For example, polycrystalline rock, including granite, exhibits brittle fracture [21]. In [22], it was shown that, in granite, microcracks are formed at the initial stage of fracture, when the breaking force does not exceed 20% of the ultimate strength. With further load increase, small cracks coalesce, and the formation of new cracks slows down. Small cracks cause a dissipation increase [20]. As one can see from the data shown in Fig. 9, in our case, the maximal change in the *Q* factor is also observed at the initial stage of fracture (presumably, at the stage of microcrack formation). By contrast, the maximal splitting of the longitudinal and flexural modes is observed under loads of 20% or more (presumably, at the stage corresponding to the microcrack coalescence and the strongest violation of symmetry in the sample).

Thus, the method of matched-filter processing allows one to extend the area of application of resonant acoustic spectroscopy to the case of materials with low *Q* factors. It becomes possible to perform acoustic measurements of viscoelastic characteristics of structurally inhomogeneous media the vibrations of which are characterized by *Q* factors within 10–20. The above results of the experimental study of fracture processes can be considered as the first step in this direction.

ACKNOWLEDGMENTS

We remember with gratitude the numerous fruitful discussions with L.M. Lyamshev. These discussions, in particular, stimulated our interest in the subject studied in this paper.

This study was supported in part by the Interdepartmental Center for Science and Engineering (project no. 1369) and the Russian Foundation for Basic

Research (project nos. 00-05-64252 and 00-15-96741). We are grateful to the Los Alamos National Laboratory (USA) for the technical support of our measurements.

REFERENCES

1. A. Migliori and J. L. Sarrao, *Resonant Ultrasound Spectroscopy: Applications to Physics, Materials Measurements, and Nondestructive Evaluation* (Wiley, New York, 1997).
2. F. Birch, J. Geophys. Res. **80**, 756 (1975).
3. J. Maynard, Phys. Today **27**, 26 (1996).
4. W. P. Mason, K. J. Marfurt, D. N. Beshers, and J. T. Kuo, J. Acoust. Soc. Am. **62**, 1206 (1977).
5. A. Migliori, W. Visscher, S. Brown, *et al.*, Phys. Rev. B **41**, 2098 (1990).
6. G. Cannelli, R. Cantelli, F. Cordero, and F. Trequattrini, Phys. Rev. B **55**, 14865 (1997).
7. P. J. Kielczynski, A. Morean, and J. F. Bussiere, J. Acoust. Soc. Am. **95**, 813 (1994).
8. J. E. Vuorinen, R. B. Schwarz, and C. McCullough, J. Acoust. Soc. Am. **108**, 574 (2000).
9. K. Foster, S. L. Fairburn, R. G. Leisure, *et al.*, J. Acoust. Soc. Am. **105**, 2663 (1999).
10. D. G. Isaak, J. D. Carnes, O. L. Anderson, and H. Oda, J. Acoust. Soc. Am. **104**, 2200 (1998).
11. H. Ogi, M. Hirao, and T. Honda, J. Acoust. Soc. Am. **98**, 458 (1995).
12. P. Heyliger and H. Ledbetter, J. Nondestruct. Eval. **17** (2), 79 (1998).
13. S. H. D. Valdes and C. Soutis, J. Sound Vibr. **228** (1), 1 (1999).
14. H. Ogi, P. Heyliger, H. Ledbetter, and S. Kim, J. Acoust. Soc. Am. **108**, 2829 (2000).
15. T. Lee, R. S. Lakes, and A. Lal, Rev. Sci. Instrum. **71** (7), 2855 (2000).
16. A. V. Lebedev, Akust. Zh. **48**, 381 (2002) [Acoust. Phys. **48**, 339 (2002)].
17. A. V. Lebedev, V. V. Bredikhin, I. A. Soustova, *et al.*, Preprint No. 588, IPF RAN (Nizhni Novgorod Inst. of Applied Physics, Russian Academy of Sciences, 2002).
18. E. Skudrzyk, *Simple and Complex Vibratory Systems* (State U.P., State College, Pennsylvania, 1968).
19. D. W. Tafts and R. Kumaresan, IEEE Trans. **70**, 975 (1982).
20. J. E. White, *Underground Sound, Application of Seismic Waves* (Elsevier, New York, 1983).
21. W. F. Brace, B. W. Paulding, and C. H. Scholtz, J. Geophys. Res. **71**, 3939 (1966).
22. T. Yanagidani, S. Ehara, O. Nishizawa, *et al.*, J. Geophys. Res. **90** (B8), 6840 (1985).

Translated by E. Golyamina